On the Feasibility of High Throughput mmWave Backhaul Networks in Urban Areas

Qiang Hu and *Douglas M. Blough*
School of Electrical and Computer Engineering, Georgia Institute of Technology

Abstract—In this paper, we investigate the design of high throughput relay-assisted millimeter-wave (mmWave) backhaul networks in urban areas. Different from most related works, we consider the deployment of dedicated simple mmWave relay devices to help enhance the line-of-sight (LoS) connectivity of the backhaul network in urban areas with abundant obstacles. Given a set of (logical) backhaul links between base stations in the network, we propose an algorithm to find high-throughput LoS paths with relays for all logical links by minimizing interference within and between paths. We also propose methods to modify the backhaul topology to increase the probability of finding high-throughput paths using our algorithm. Extensive simulations, based on a 3-D model of a section of downtown Atlanta, demonstrate that high-throughput topologies, with minimal inter-path and intra-path interference, are feasible in most cases. The analyses also yield some insights on the mmWave backhaul network design problem.

I. INTRODUCTION

5G networks are expected to deploy smaller cells containing a much larger number of base stations (BSs) as compared to 4G networks. However, small-cell deployment in dense urban areas will face a severe backhaul challenge, wherein a huge amount of data needs to be transmitted between the many BSs. In this paper, we focus on the backhaul connecting the small-cell BSs within a single macro-cell region. Due to the prohibitive cost and construction limits, it may not be possible to establish wired fiber connections between all BSs in dense urban areas. Thus, wireless backhaul becomes an attractive solution to this challenge, because of its more flexible deployment and lower cost. In particular, millimeter-wave (mmWave) backhaul is very promising due to above 10 Gbps achievable data rates on mmWave links.

Most related work on mmWave backhaul in the dense urban environment adopts a *self-backhaul* architecture, where BSs connect to each other directly through mmWave wireless links. However, due to the well-known *blockage effect* of mmWave signals, when LoS connections between BSs do not exist, non LoS signaling paths cannot support the high data rates required for backhaul traffic. Since the deployment of BSs typically focuses on maximizing cellular coverage, mmWave small-cell BSs will likely be mounted at lower heights. This will make it even more difficult to find LoS connections between small-cell BSs due to the abundant obstacles in dense urban areas. As an example, through simulations on the 3-D topology of downtown Atlanta shown in Fig. 1, we found that only 42% of base station pairs had LoS connections.

To address the above issues, we propose to deploy simple and cheap dedicated mmWave relays on the surfaces of buildings to build a relay-assisted mmWave backhaul in dense urban areas as shown in Fig. 1. With the deployment of relays, high throughput multi-hop paths, where every mmWave physical link is LoS, can be formed where direct LoS links between BSs are not available. Furthermore, the introduction of relays brings the benefit of better utilizing the space diversity, which plays an important role in minimizing mutual interference. In [1], the authors present an optimal relay selection and scheduling scheme for a single backhaul link. However, if relays for multiple backhaul links are chosen without coordination, several links may "share" some relays, which is not allowed as we assume each mmWave relay is dedicated to a single backhaul link. Moreover, the issue of "inter-path" mutual interference arises when multiple relaying paths co-exist in the same area. Mutual interference must be carefully dealt with, otherwise the performance of the whole system could degrade severely.
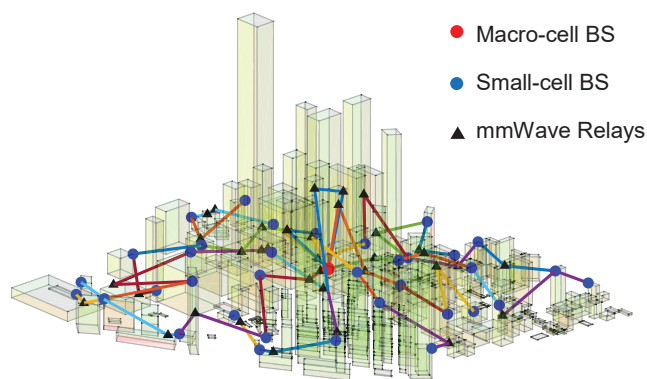

Fig. 1. A relay assisted mmWave backhaul network in downtown Atlanta.

In this paper, our contributions are summarized as follows:

- we present the first algorithm for relay selection across an entire mmWave backhaul network containing multiple logical links and accounting for interference between different physical links,
- through extensive simulation results based on a 3-D model of a section of downtown Atlanta, we demonstrate that our algorithm can find interference-minimal high-throughput paths for all logical links comprising a backhaul network topology,
- we propose two topology modification methods and show that they increase the probability of finding interference-minimal paths to above 95% even in certain problematic scenarios, thus demonstrating the feasibility of high-throughput mmWave backhaul, and

- we demonstrate, through simulations, that the use of relays at least quadruples the aggregate traffic demand that can be met with our approach as compared to a self-backhaul network without relays.

II. RELATED WORK

In [2], Samsung proposed the point-to-multi-point (P2MP) "in-band" mmWave backhaul networks, where a single macro-cell BS serves as the gateway node for several small-cell BSs to the backbone Internet, and the inter-BS communications are supported by mmWave wireless links. "In-band" means that backhaul and access transmissions are multiplexed on the same frequency band. [3], [4] deal with the multi-hop tree/mesh-like mmWave P2MP backhaul network. All these works focus on finding the time-division-multiplexing (TDM) based schedule of backhaul links, so that the backhaul system performance can be optimized in terms of different metrics, such as throughput and QoS. The term of "relaying" also appears in many "self-backhaul" related works [5]–[9]; however, it only refers to the functionality of intermediate BSs along the multi-hop paths, which is quite different from our work, as we consider dedicated mmWave relay devices deployed in the backhaul. In [8], the authors proposed a multi-hop mmWave self-backhaul in the street canyon scenario. Orthogonal frequency based schedule is used to control the mutual interference, which limits the scale of the linear backhaul network and the throughput is not very high. Moreover, [9]–[11] focus on optimizing the throughput or robustness performance for the mmWave backhaul in the roadside scenarios; however, it is different from the general dense urban scenario we use here, which has abundant obstacles easily blocking LoS paths between wireless nodes.

III. SYSTEM MODEL

Point-to-multipoint mmWave backhaul in 3-D urban areas: To capture more practical features of the dense urban outdoor environment, we build a three-dimensional (3-D) model of downtown Atlanta, GA and use it throughout the paper. Note that the following problem analysis and proposed algorithms are not subject to the specific city model in use. In the 3-D model, buildings are modeled as cuboids for simplicity. To form "small-cells", we partition the modeled urban area into square grids with side length l_g. Within each small cell (i.e., grid), only one small-cell BS is deployed on a randomly selected top vertex of a building, except that in the central small cell, a macro-cell BS with wired backhaul connection is deployed. In our problem, a single macro-cell BS serves as the gateway node of small-cell BSs to the backbone Internet.

Backhaul topology: A set of *logical links* between BSs are defined in the backhaul topology, so that each small-cell BS has a route, either single-hop or multi-hop, to the macro-cell BS. We propose a simple tree-based backhaul topology to support the assumed backhaul traffic model, with each small cell having a total traffic demand of D Gbps. Here we omit the details of the topology generation algorithm due to limited space. In fact, the backhaul topology can be either tree- or

mesh-style, and in this paper, we choose to start from the simpler tree case and leave the mesh case as future work. Fig. 2 shows an example mmWave backhaul topology with 1 macro-cell BS and 21 small-cell BSs in the downtown Atlanta area. Fig. 2a is the abstract topology in grids ($l_g = 300$ m) and the numbers are the minimum rate requirement of each backhaul logical link; while Fig. 2b is the 2-D view of this topology in the 3-D modeled area. We assume enough radio chains are available on each BS, so that multiple logical links attached to a BS can transmit and receive simultaneously. Note that logical links closer to the macro-cell BS have higher link rate requirement, because the logical link between a parent BS and a child BS has to support the data traffic required by all nodes in the child BS's sub-tree. Moreover, as the downlink and uplink data traffic can be simply scheduled in a time-division way using the same backhaul network, we only focus on the downlink case in the rest of this paper.
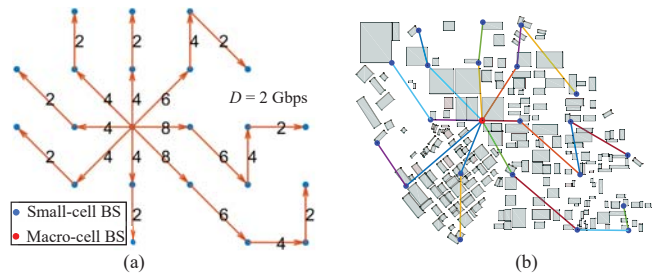

Fig. 2. An example of mmWave backhaul topology ($D = 2$ Gbps)

Relay-assisted mmWave backhaul network: In the backhaul network, dedicated mmWave relays are used to form a multi-hop multi-Gbps path for a logical link wherever a direct LoS link between the end BSs is not available. Here "dedicated" means one relay can only be used to support one logical link. To lower the cost, we assume relays are simple devices that cannot support sharing between different logical links. To model the constraints of deploying relays in the real world, we assume a set of feasible candidate relay locations is given, and a subset of these locations will be used for actual relays in the backhaul network.

Interference issues: We assume *primary* interference does not allow a mmWave relay to transmit and receive simultaneously. However, as BSs are more powerful and complex devices, multiple logical links connected to the same BS can actively transmit data at the same time, as long as the *secondary mutual* interference among them is avoided. Mutual interference comes from the concurrent transmissions of different wireless *physical links* in the network. It is commonly assumed that LoS mutual interference is dominant in random mmWave ad-hoc networks with high-gain highly directional antennas and abundant obstacles in the environment, and the aggregated non LoS interference is negligible [12]. Thus, in this paper, we do not explicitly consider the mutual interference produced by the reflected signals, which experience much larger path loss due to the longer propagation distance and extra reflection attenuation against building surfaces. Moreover, as we deploy the back-

haul network in a 3-D environment, usually the physical links are not in the horizontal plane, so that the reflected signals are likely pointing to either the sky or the ground, making them unlikely to affect receivers with narrow beam directional antennas. In our approach, when relays are selected to form different logical links, *space diversity* is exploited to minimize the (LoS) mutual interference among physical links in the network.[1] We use a sectored antenna model [12]. The antenna gain is G_h within the main beam with a beam width B; while it is G_l outside the main beam.

IV. MULTI-PATH SELECTION FOR RELAY-ASSISTED MMWAVE BACKHAUL NETWORKS

As the backhaul topology only defines the set of logical links, we still need to determine how to establish these multi-Gbps logical links. In our relay-assisted approach, we select some candidate relay locations to deploy mmWave relays for each logical link in the topology. In this way, a logical link is constructed upon either a single-hop LoS path, or a multi-hop relaying path. Different from the problem in [1], in our problem, multiple logical links need to be constructed together, and the aim is to jointly optimize the relay selection within different logical links so that they can achieve their given throughput requirements.

To maintain a high signal-to-interference-and-noise-ratio (SINR) value at each receiver, strong secondary mutual interference should not exist when concurrent transmissions among multiple physical links happen. However, the algorithm in [1] only considers controlling the intra-path interference; while in this work, we have to take both intra- and inter-path mutual interference into account. Besides the interference issue, if multiple paths are selected independently, it may result in relay sharing between different paths, which breaks the dedicated relay assumption mentioned earlier. Thus, we have to avoid the intersection between different relaying paths. In fact, we can formulate this problem as a Boolean Satisfiability Problem, and problems of that type are typically NP-Complete. Considering the problem size and complexity, we propose heuristic algorithms to address it.

A. Interference-and-relay-sharing-avoidance multi-path construction algorithm

We propose an interference-controlled multi-path searching algorithm for constructing relay-assisted mmWave backhaul networks in dense urban areas, which is described by Algorithm 1. Paths are searched one after another, with an efficient method of switching sequences of logical links when an interference-minimal and no-relay-sharing path for a logical link cannot be found in its current sequence. This process ends when either paths are all found for all backhaul links or there is "no solution found".

The variables used in the algorithm are the the given set of logical links $\mathcal{L}$, the two-dimensional list $\mathcal{N}$ where each

---

[1]Time or frequency division based schemes can be used to avoid the mutual interference, which sacrifice the throughput performance as either time or frequency resource cannot be fully utilized.

row i records the LoS neighbors of node i in the network, the number of hops h within a logical link, whose upper bound is H, the maximum length L_m of a physical link aiming to guarantee a minimum physical link capacity, a binary variable ns indicating "no solution" of the algorithm when it is false, and two lists R_s and P_s recording the selected relays and physical links, respectively. Each logical link object has the following attributes: $\{s, d, th_m, seq, path, links\}$, which represent the source BS, destination BS, the minimum required throughput, the initial sequence number, the nodes along the path, and the selected physical links, respectively.

Algorithm 1 Multi-path selection algorithm

Input: $\mathcal{L}, H, L_m, \mathcal{N}$
Output: $\mathcal{L}$
1:   $ns \leftarrow$ **false**; $R_s \leftarrow \varnothing$; $P_s \leftarrow \varnothing$;
2:   **for** $j \leftarrow 0$ to $|\mathcal{L}| - 1$ **do**
3:     **if** ns **then**
4:       **return** $\varnothing$;
5:     $h \leftarrow 1$; $\mathcal{L}[j].path \leftarrow \varnothing$; $\mathcal{L}[j].links \leftarrow \varnothing$;
6:     **while** $\mathcal{L}[j].path = \varnothing$ **do**
7:       **if** $h > H$ **then**
8:         find $\max_{k<j} k$, such that $\mathcal{L}[k].seq < \mathcal{L}[j].seq$;
9:         **if** $k \geq 0$ **then**
10:          switch $\mathcal{L}[k]$ and $\mathcal{L}[j]$ in $\mathcal{L}$;
11:          $R_s \leftarrow \varnothing$; $P_s \leftarrow \varnothing$; $j \leftarrow 0$;
12:         **else**
13:          $ns \leftarrow$ **true**;
14:         **break**;
15:       findNextNode($L[j], h, \mathcal{N}, L_m, 100, \{l.s\}, P_s, R_s$);
16:       **if** $L[j].path \neq \varnothing$ **then**
17:         $R_s \leftarrow R_s \bigcup L[j].path(1 : end - 1)$;
18:         $P_s \leftarrow P_s \bigcup L[j].links$
19:     $h \leftarrow h + 1$;
20: **return** $\mathcal{L}$;

When $h > H$, it indicates that an interference-minimal and no-relay-sharing path for a logical link cannot be found in its current sequence through the method "*findNextNode*", which is a depth-first single-path searching algorithm summarized in Algorithm 2. It also triggers the procedure of switching sequences of logical links (line 8-11) . We move the problematic logical link $\mathcal{L}[j]$ forward through switching it with the closest link $\mathcal{L}[k]$ in the list $\mathcal{L}$ before $\mathcal{L}[j]$, which has a smaller *seq* value than $\mathcal{L}[j]$'s. This method make sure to avoid infinite loop. When a switch occurs, the multi-path search restarts.

When no previous logical link is available to switch with the problematic link, the algorithm reports "no solution found" (line 13). On the other hand, when all paths are found, it returns the updated $\mathcal{L}$.

B. Interference-and-relay-sharing-avoid single-path searching algorithm

Different from [1], the single-path searching Algorithm 2 in this work has to additionally consider inter-path interference and avoid sharing relays between different logical links.

The variables defined in Algorithm 2 are the logical link object l, the maximum number of hops h_m, the current $path$ (i.e., a list of selected nodes) and the capacity cap_p of the latest selected physical link.

The searching only starts when the current hop $h_c <= h_m$ and no path has been found for l (line 2-3). The algorithm

---

Algorithm 2 findNextNode() for single path selection

Input: $l, h_m, \mathcal{N}, L_m, cap_p, path, P_s, R_s$
1: $h_c \leftarrow |path|$;
2: **if** $h_c > h_m \vee l.path \neq \varnothing$ **then**
3:    **return**
4: $n_p \leftarrow path.back()$; $N_c \leftarrow \mathcal{N}[n_p]$;
5: **for** n_c in N_c **do**
6:    **if** n_c is a BS $\wedge$ $n_c \neq l.d$ **then**
7:      **continue**;
8:    **if** $n_c \in R_s \vee n_c \in path$ **then**
9:      **continue**;
10:   $dist_c \leftarrow \|n_c - n_p\|$; $dist_d \leftarrow \|l.d - n_c\|$;
11:   **if** $dist_d > (h_m - h_c)L_m \vee dist_c > L_m$ **then**
12:     **continue**;
13:   $cap_c \leftarrow \text{dist2cap}(dist_c)$;
14:   $cap_{cp} \leftarrow cap_p cap_c (cap_p + cap_c)^{-1}$;
15:   **if** $cap_{cp} < l.th_{min}$ **then**
16:     **continue**;
17:   $intra \leftarrow \text{intraINFCheck}(n_c, n_p, path)$;
18:   $inter \leftarrow \text{interINFCheck}(n_c, n_p, P_s)$
19:   **if** $intra \vee inter$ **then**
20:     **continue**;
21:   $path.push(n_c)$;
22:   **if** $n_c = l.d$ **then**
23:     $l.path \leftarrow path$;
24:   **else**
25:     findNextNode$(l, h_m, \mathcal{N}, dist_m, cap_c, path, P_s, R_s)$;

---

iterates every neighbor of the latest selected node n_p in the $path$ to check whether it is a qualified node for the current hop n_c. Since we do not allow other BSs to appear as "relays" in a logical link, they are filtered (line 7-9). To avoid relay sharing, a relay n_c that has already been selected by other logical links or by the current $path$ is neglected. As a crucial step of reducing the running time of the algorithm, line 13-16 restricts the scale of the depth-first search by discarding n_c when the physical link from n_p to n_c is too long or the distance from n_c to the destination $l.d$ cannot be covered by the remaining hops.

If n_c is still "alive", the capacity of current hop cap_c is estimated by calling a function "dist2cap", which uses the Friis transmission equation and Shannon's capacity formula to calculate capacity from link length with other parameters fixed for a given network scenario. Our prior work showed that the bottleneck of a multi-hop logical link is determined by the consecutive link pair with the minimum end-to-end throughput [1]. Accordingly, Line 15 checks to make sure that the end-to-end throughput of the current consecutive link pair cap_{cp} is larger than the throughput demand $l.th_m$.

Next, the current candidate physical link has to pass both intra- and inter-path interference checks (Line 17–18) before n_c is appended as a new node in $path$. Both interference checking functions are designed based on our simplified interference model, which is described in the next subsection. If n_c is the destination, $path$ is officially assigned to l; otherwise, the procedure calls "findNextNode" again to continue searching.

The time complexity of Algorithm 2 is $O(M^h)$, where M is the maximum degree of the LoS connectivity graph of candidate relay locations and h is the number of hops in a logical link. Since M and h are both small numbers, the algorithm runs quite fast in practice. We also note that the algorithm is run at network deployment time, not during network operation, which makes running time less critical.

C. Avoiding mutual interference with a simplified model

Typically, upon the interference analysis in wireless networks, either physical or protocol interference model [13] is in use; however, physical model is hard to apply in the one-by-one relay selection process, as we cannot obtain the accurate amount of interference at each receiver until the whole process ends. Thus, in this work, upon the system assumption and the sectored antenna model in use, we adopt a simplified model to determine the interference relationship between different physical links in the network, which can be easily incorporated into our proposed multi-path searching algorithm.
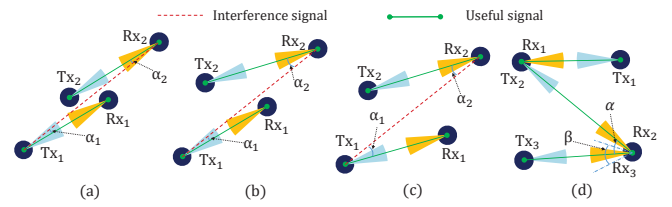

Fig. 3. Interference conditions

The amount of mutual interference significantly varies according to the positioning relationship between different physical links. Fig. 3 (a-c) shows three different interfering cases between two disjoint physical links. Despite the 2D depiction in the figure, all simulations were performed with consideration of 3D antenna beams. When the angle between the directions of useful signal and interference signal (i.e., α_1 and α_2) is smaller than half of the beam width $\frac{B}{2}$, the interference is amplified by G_h; otherwise, it is amplified by G_l. (a) indicates the "*most-interfered*" case, where the interference signal from Tx_1 to Rx_2 is amplified by the high antenna G_h at both ends. The "*medium-interfered*" case is shown in (b), where the interference signal is only amplified by G_h once at either end. When the interference signal experiences G_l at both ends, as depicted in (c), the amount of interference becomes extremely low, and this case is considered as "*least interfered*". During the path selection process, we aim to form different physical links which have the least-interfered relationship between each other.

When two physical links share one end node (which can only be a BS in our architecture), the analysis of mutual interference involves two cases, as shown in Fig. 3 (d). First, when the two antennas on the BS are transmitting and receiving simultaneously (i.e., Tx_2 and Rx_1), this is a special case where interference is very high due to the receiver being so close to the transmitter. For simplicity, we assume that as long as their main beams do not overlap (i.e., $\alpha > B$), the isolation between antennas is large enough to handle the mutual interference. Actually, this case can be avoided through scheduling also, which is not the focus of this paper. However, when two antennas on the BS are receiving at the same time, it is the "medium-interfered" case according to Fig. 3 (b). Nevertheless, considering BSs could have better antenna design and advanced antenna isolation technology, we assume that as long as the angle α between two physical links is larger than a threshold value β, the "medium-interfered" case at BSs is also acceptable during path searching. In fact, in the downlink, this case does not occur.

In fact, the relay-assisted mmWave backhaul network shown in Figure 1 is drawn based on the path data obtained from the simulation where using our proposed algorithm can successfully construct all required logical links defined in the backhaul topology.

V. SIMULATION RESULTS AND ANALYSIS

In this section, we explain the simulations conducted to evaluate the performance of our proposed algorithms. Table I summarizes the system parameters used in our simulations. 227 buildings higher than 5m are modeled in the $1200 \times 1600 \ m^2$ area, which is larger than a typical 4G macro-cell in a dense urban environment (see Fig. 1 and Fig. 2).

TABLE I
SIMULATION PARAMETERS

Symbol	Value	description
l_g	300, 200 m	grid/cell size (side length)
l_p	300 m	maximum physical link length
n_{rm}	1,2,3	minimum number of relays per surface
σ_r	$n_{rm} \times 10^{-4}/m^2$	density of extra relays
h_t	50 m	maximum height for BSs
G_h	21.40 dBi	antenna gain of main lobe
$G_h - G_l$	20-40 dBi	antenna gain isolation
β	30°	antenna isolation angle
B	$5^o - 15^o$	beam width
f_c	60 GHz	carrier frequency
BW	2.16 GHz	channel bandwidth
D	2 Gbps	traffic demand of each small cell BS
p_t	1 watt	transmit power
α	16 dB/km	atmosphere attenuation
η	2.0	path loss exponent
m_l	10 dB	link margin

A. Feasibility of high-throughput mmWave backhaul

We first run the multi-path selection algorithm with different antenna beam widths, candidate relay densities, and a grid size of 300m (i.e., $22 - 23$ BSs). For each parameter setting, the simulation runs 100 times. For each run, we generate a new mmWave backhaul topology on a new set of randomly selected BSs and with a new set of candidate relay locations in the modeled macro-cell region. As we modify the parameters n_{rm} and σ_r, the total number of candidate relay locations varies among $\{1152, 2384, 3644\}$. Note that, without relays, the lack of LoS links between BS pairs makes it impossible to support 2 Gbps traffic demand on each BS.

Fig. 4 shows that, in many cases, the use of relays enables a high-throughput backhaul network to be formed. To be specific, when the beam width is small (e.g., 5°–9°), more than 90% of the time, we find a set of paths with required capacity and physical links that only experience the "least-interfered" case to build a relay-assisted mmWave backhaul network. As more candidate relay locations are added, the feasibility of backhaul network construction increases, due to the extra available space diversity brought by the additional candidate relay locations. However, as the antenna beam width increases, the feasibility using Algorithm 2 decreases, because the wider beams produce larger interference regions.
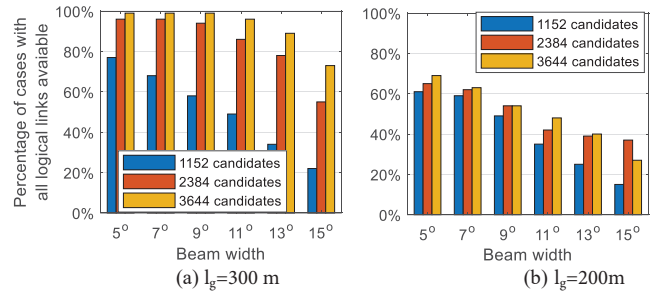

Fig. 4. Probability of finding feasible paths for all logical links.

To further investigate feasibility, we "shrink" the size of each small cell by setting $l_g = 200 \ m$, which results in more small cells (i.e., $37 - 41$ BSs) and correspondingly more backhaul logical links. As the cell size is almost halved, we set the traffic demand of each small cell BS to $\frac{D}{2}$ Gbps. As shown in Fig. 4 (b), the percentage of feasible network scenarios drops substantially, and even when the beam width is 5°, it is below 70%. The reasons for this drop are: 1) the space diversity at the macro-cell BS may not be enough to support 8 logical links connecting to it,[2] 2) too many logical links have to be constructed within the overall area, which produces large interference regions, limited space diversity, and more severe relay contention, and 3) the modeled macro-cell area is not symmetric, i.e. as more small cell BSs appear, the generated backhaul topology becomes even more unbalanced leading to some "hot" logical links with much higher throughput requirement than others near the macro-cell BS. To address these issues, we consider modifying the topology generating process by either macro-cell BS splitting or macro-cell shrinking, which are described next.

1) *Macro-cell BS splitting*: To address the insufficient space diversity issue, we propose to "split" the macro-cell BS by

---

[2]We tested the maximum number of physical links from the macro-cell BS that will not interfere with each other using the Bron-Kerbosch algorithm [14] and found that in more than 30% of the total simulated cases, the space diversity at the macro-cell BS cannot support 8 links

adding another radio head (see Fig. 5 (a)) to the BS. The extra radio head is mounted at a higher level, and connected to the BS through a wired connection. Each radio head handles half of the logical links at the macro-cell BS, which reduces the space diversity requirement on each radio head.

2) *Macro-cell shrinking*: In fact, the modeled area is much larger than the typical size of a 4G macro-cell in a dense urban environment. Thus, we re-size the interested macro-cell to a $1000 \times 1000 \ m^2$ area, where the macro-cell is located at the center (see Fig. 5 (b)). In this way, the number of logical links within a macro-cell is reduced to around 23, and the traffic requirement of logical links is also reduced.
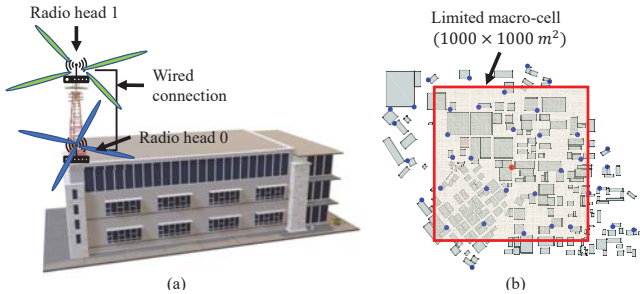

Fig. 5. Methods to improve the backhaul topology

We apply method 1) to the simulations with $l_g = 300 \ m$, and apply both method 1) and 2) to the simulations with $l_g = 200 \ m$. Fig. 6 shows that mmWave backhaul feasibility with $l_g = 200 \ m$ is greatly improved using a combination of the two proposed methods, and the likelihood of finding feasible paths for all logical links in the topology is above 90% when the antenna beam width is not larger than 11°. The "macro-cell BS splitting" method works fairly well in narrow beam cases; however, when the beam width is large (i.e., 15°), to achieve favorable performance, we need to control the size of a macro-cell. It is also noticed that, when the first method is applied in the $l_g = 300 \ m$ case, as long as the beam width is not larger than 13°, the likelihood of finding a feasible solution using our algorithm is above 95%.
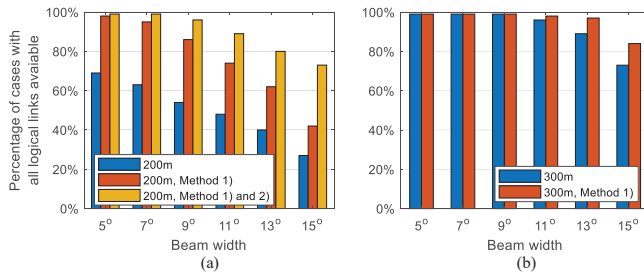

Fig. 6. Updated probability of finding feasible paths for all logical links (3644 candidate relays)

The above discussion indicates that if the density of small cell BSs is high, to increase the feasibility of a mmWave backhaul in dense urban areas, the size of a macro-cell has to be controlled so that single macro-cell BS does not have to support too many small cell BSs. Moreover, the backhaul topology is expected to be balanced, so that the number of hops from a edge BS to the macro-cell BS is not too large.

B. Throughput performance

In the above simulations, we set the traffic demand D at each small cell BS to be 2 Gbps, and all feasible solutions satisfy the aggregate demand. To get more insight on backhaul performance, we show the maximum achievable aggregated traffic demand at the macro-cell BS in both relay-assisted-backhaul and self-backhaul networks. To evaluate the capacity of each logical link, we use the 3GPP UMi Street Canyon pathloss model, which is also used in [8]. We focus on two scenarios, i.e., $l_g = 300m$ and $l_g = 200m$ with limited macro-cell size, where relay-assisted backhaul is highly feasible. As shown in Fig. 7, in both scenarios, the median of the maximum aggregated traffic demand of all feasible relay-assisted backhaul networks is 66.1 and 60.9 Gbps; while the value drops to 3.1 and 15.2 Gbps for the self-backhaul solution. Thus, the use of relays to produce LoS connections at least quadruples the aggregate traffic demand that can be met with a mmWave backhaul deployment in the simulated scenarios. The figure also shows that relay-assisted backhaul does better with a larger cell size; while self-backhaul prefers a smaller cell size, since longer distance of logical links leads to lower LoS probability and larger path loss.
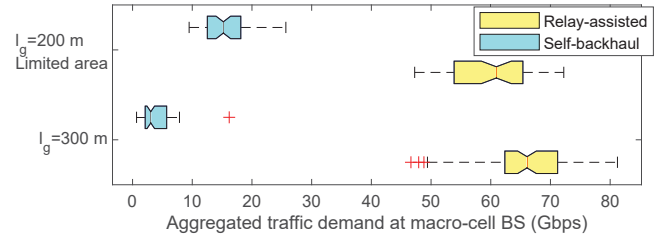

Fig. 7. Maximum achievable aggregated traffic demand at macro-cell BS

C. The number of relays used in the mmWave backhaul

While feasibility of the network is our primary concern, we are also interested in how efficient the constructed networks are in terms of the number of relays that need to be deployed. Note that a lower bound on the total number of relays required can be found by running the optimal single path selection algorithm from [1] for each path independently.
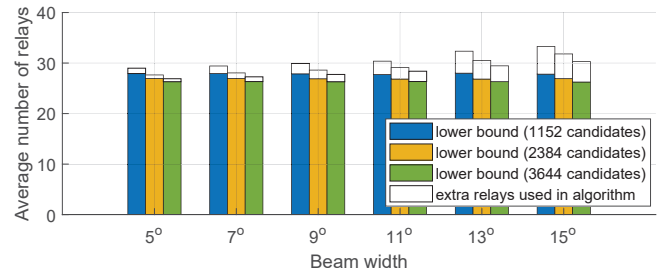

Fig. 8. The number of relays used ($l_g = 300$ m)

As shown in Fig. 8, on average, about 27-33 relays are used by 21-23 paths in our algorithm. As the beam width increases, a few more relays are needed to help control the mutual interference in the network. We can reduce the number of relays needed by increasing the number of candidate relay locations in the backhaul area. The number of relays deployed is fairly close to the calculated lower bound, especially when the beam width is no larger than 11°.

D. Accuracy of the simplified interference model

To evaluate the accuracy of our simplified interference model, we took the final topologies and calculated the mutual interference at the receiver of each physical link using the physical interference model. Fig. 9 shows the cumulative distribution functions (CDF) of the path throughput degradation when the more accurate physical interference model is used and for different antenna main-beam-to-side-lobe-ratios (AMSR). In all figures, a larger AMSR means smaller throughput degradation. Fig. 9(a) shows the throughput degradation when the transmissions on multiple links at a BS are intelligently scheduled, and no two links on the same BS are simultaneously receiving, or simultaneously transmitting and receiving. In this case, we see that the simplified interference model is very accurate for $\geq$ 25 dB AMSR, which is typical with state-of-the-art antennas. Fig. 9(b) shows the situation when multiple links on the same BS are used simultaneously but there is near-perfect isolation (i.e., $>$ 120 dB) between antennas. Although the throughput performance is still good in this case, it drops somewhat because the large antenna isolation only eliminates the interference due to two antennas transmitting and receiving simultaneously while the interference due to two antennas receiving at the same time still hurts the throughput. The largest performance drop occurs in Fig. 9(c), where we assume leakage of -80 dBm between every pair of antennas transmitting and receiving simultaneously on the same BS, and we can see that there is additional throughput degradation that cannot be eliminated by increasing AMSR.
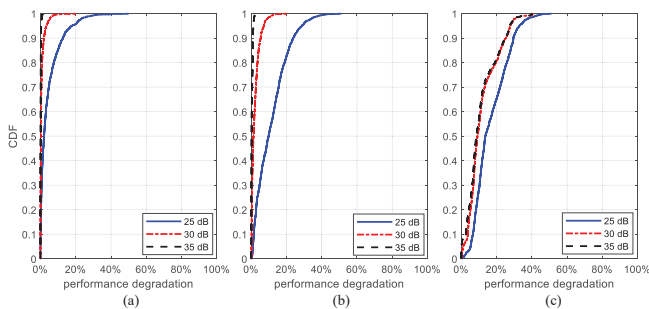

Fig. 9. Throughput performance degradation with more accurate interference model for different main beam to side lobe ratios ($l_g = 300$ m, $B = 15^o$)

VI. Conclusion

In this paper, we propose a multi-path construction algorithm which can be used to form all required logical links

defined in a relay-assisted mmWave backhaul network in the urban environment. To the best of our knowledge, we are the first to address this problem. Simulations based on the 3D modeling of downtown Atlanta area show that the high feasibility of constructing an interference-minimal relay-assisted backhaul network can be achieved, through applying several enhancing methods on the system. Fig. 9 indicates that antenna isolation is the most crucial factor in maintaining the throughput required for backhaul networks. Absent good antenna isolation, intelligent network-level scheduling will be required to optimize network throughput, although its performance is upper bounded by the results shown here with good antenna isolation and minimized interference. Network-level scheduling is the subject of our current research.

REFERENCES

[1] Q. Hu and D. Blough. "Relay selection and scheduling for millimeter wave backhaul in urban environments." *2017 IEEE 14th International Conference on Mobile Ad Hoc and Sensor Systems (MASS)*, IEEE, 2017.

[2] R. Taori and A. Sridharan. "Point-to-multipoint in-band mmWave backhaul for 5G networks." *IEEE Communications Magazine*, 53.1 (2015): 195-201.

[3] K. Zheng, L. Zhao, J. Mei, M. Dohler, W. Xiang, and Y. Peng. "10 Gb/s hetnets with millimeter-wave communications: access and networking-challenges and protocols." *IEEE Communications Magazine*, 53.1 (2015): 222-231.

[4] Y. Zhu, Y. Niu, J. Li, D. Wu, Y. Li, and D. Jin. "QoS-aware scheduling for small cell millimeter wave mesh backhaul." *2016 IEEE International Conference on Communications (ICC)*, IEEE, 2016.

[5] S. Singh, M. Kulkarni, A. Ghosh, and J. Andrews. "Tractable model for rate in self-backhauled millimeter wave cellular networks." *IEEE Journal on Selected Areas in Communications*, 33.10 (2015): 2196-2211.

[6] A. Ahmed and D. Grace. "A dual-hop backhaul network architecture for 5g ultra-small cells using millimeter-wave." *2015 IEEE International Conference on Ubiquitous Wireless Broadband (ICUWB)*, IEEE, 2015.

[7] R. Ford, F. Gomez-Cuba, M. Mezzavilla, and S. Rangan. "Dynamic time-domain duplexing for self-backhauled millimeter wave cellular networks." *2015 IEEE International Conference on Communication Workshop (ICCW)*, IEEE, 2015.

[8] J. Du, E. Onaran, D. Chizhik, S. Venkatesan, and R. Valenzuela. "Gbps user rates using mmWave relayed backhaul with high-gain antennas." *IEEE Journal on Selected Areas in Communications*, 35.6 (2017): 1363-1372.

[9] M. Kulkarni, A. Ghosh, and J. Andrews. "Max-min rates in self-backhauled millimeter wave cellular networks." *arXiv preprint* arXiv:1805.01040 (2018).

[10] Q. Hu and D. Blough. "Optimizing millimeter-wave backhaul networks in roadside environments." *2018 IEEE International Conference on Communications (ICC)*, IEEE, 2018.

[11] Y. Liu, Q. Hu, and D. Blough, "Blockage Avoidance in Relay Paths for Roadside mmWave Backhaul Networks," *2018 IEEE 29th Annual International Symposium on Personal, Indoor and Mobile Radio Communications (PIMRC)*, IEEE, 2018.

[12] A. Thornburg, T. Bai, and R. Heath. "Interference statistics in a random mmWave ad hoc network." *2015 IEEE International Conference on Acoustics, Speech and Signal Processing (ICASSP)*, IEEE, 2015.

[13] P. Gupta and P. Kumar. "The capacity of wireless networks." *IEEE Transactions on information theory*, 46.2 (2000): 388-404.

[14] C. Bron and J. Kerbosch. "Algorithm 457: finding all cliques of an undirected graph." *Communications of the ACM,* 16.9 (1973): 575-577.